Hermetic RF Feedthroughs for Probing Hydrogen Absorbed Palladium Nanomechanical Resonators at Cryogenic Temperatures

Abhishek Kumar

A dissertation submitted for the partial fulfilment

of a BS-MS dual degree in Science

Indian Institute of Science Education and Research Mohali

April 2014

Certificate of Examination

This is to certify that the dissertation titled "**Hermetic RF feedthroughs for probing hydrogen absorbed palladium nanomechanical resonators at cryogenic temperatures**" submitted by **Abhishek Kumar** (Reg. No. MS09004) for the partial fulfillment of BS-MS dual degree programme of the Institute, has been examined by the thesis committee duly appointed by the Institute. The committee finds the work done by the candidate satisfactory and recommends that the report be accepted.

Dr. Yogesh Singh Dr. Sudeshna Sinha Dr. Ananth Venkatesan
(Supervisor)

Dated: April 25, 2014

Declaration

The work presented in this dissertation has been carried out by me under the guidance of Dr. Ananth Venkatesan at the Indian Institute of Science Education and Research Mohali.

This work has not been submitted in part or in full for a degree, a diploma, or a fellowship to any other university or institute. Every effort has been made to acknowledge contributions of fellow researchers wherever applicable. This thesis is a bonafide record of original work done by me and all sources listed within have been detailed in the bibliography.

Abhishek Kumar
(Candidate)

Dated: April 25, 2014

In my capacity as the supervisor of the candidate's project work, I certify that the above statements by the candidate are true to the best of my knowledge.

Dr. Ananth Venkatesan
(Supervisor)

Acknowledgments

Help and support from a lot of people have resulted in the completion of this project. And it is not possible to do true justice to all of them. But I will try my best to mention any supporting hands that came into way.

I would like to express my heartiest gratitude to my supervisor Dr. Ananth venkatesan, who gave me the opportunity to work on this project with him. His experience, insight and guidance taught me a great deal while doing the project.

Suggestions and directions given by Shishram Rebari and Indrajeet, who were involved with various other aspects of the project before I joined them, helped me a lot figuring out various obstacles that came in my way.

A proper environment is necessary for working in a lab, and I am thankful to my labmates: Shubhendu, Rakesh, Inderjeet and Dr. Satyendra for maintaining such a friendly environment in the lab and also for lending a helping hand whenever necessary. I am also thankful to our neighbouring lab people, for having such a great aura around.

I would also like to thank Mr. Vinod for machining various pieces of brass and copper in his workshop and for suggesting various modifications in the drawing which led to better functioning of the components. I am also thankful to Mr. Ramprasad from Ramdarbar area of Chandigarh for teaching me brazing techniques.

The palladium sample used, were fabricated in the semiconductor fabrication facility at the University of Regensburg, Germany, and I would like to thank Prof. D. Weiss for allowing Dr. Venkatesan to use the facility.

Stycast used for sealing all components were prepared in a lab adjacant to us and I am thankful to Dr. Goutam Sheet for allowing me to use fumehood in his lab.

I would also like to thank my colleagues, Ravi, Jithin, CR (OK...Abhishek Anand), Ankush, Mayank, Shivpal, Katu and so many others that it is not possible to put everyone's name, for such a great and wonderful five years of college life at IISER Mohali. I am also thankful to our college for bringing us all together from various parts of the country and making us such good friends.

The INSPIRE fellowship since 2009 played an important role in meeting my financial needs and I am grateful to Department of Science and Technology, Government of India for that.

Last, but not the least, I would like to aknowledge my parents and sister Anshu for their love and support. None of this would have been possible without their unconditional love, care, hard work and sacrifice to allow me to come here and fulfill my dreams.

Contents

List of Figures

Abstract

With the development of nanotechnology within the last few decades, miniaturization of a lot of electromechanical devices has taken place. The nano scale devices have potentials not only to serve for a variety of applications, but can also play an important role in unraveling interesting fundamental physics. Introduction of such devices to ultra low temperatures, where the state of device is not dominated by its thermal energy any more, further increases the expectations to observe interesting quantum phenomenons.

In this thesis, we shall focus on nanoelectromechanical resonators at cryogenic temperatures. We have already studied low temperature dissipation in a nano-scale palladium beam of dimensions approximately 5 micron long, 200 nm wide & 80 nm thick and measured resonance frequency of around 34 MHz. To modify the behaviour and further understand physical properties of the two level system with absorbed Hydrogen, a vacuum can is fabricated for the dilution fridge with hermetic DC and radio-frequency feed-throughs to be used at cryogenic temperatures (as low as 10mK). A novel hermetic feed through is developed for high frequency signal communications at cryogenic temperatures with minimal modification to commercially available glass bead equipped SMA. A brief section discussing the theory behind the resonator at low temperature, and in the presence of absorbed hydrogen is also discussed, along with the basic theory of operation of dilution refrigerator.

Chapter 1

Introduction and Theory

The importance of resonators in our everyday life is immense, and can't be neglected. Nature itself provides us with ear drums, a resonator as detector and vocal chord, a resonator as source, which enables us to interact through voice and speech. Any sound that we hear, are produced somewhere through some resonator.

We have come a long way from there, developing man-made resonators which play an unaccountable role in human world like in musical instruments, electronic circuits etc. However, with the development of nanotechnology within the last few decades, we have taken another step forward towards nanomechanical resonators.

Not only that, researches have shown a wide range of applications where it can be implemented. Eom (Eom et al. 2011) has mentiond a lots of nanoelectromechanical resonator's applicability in nanoscale sensing and detection (**Craighead2000**) (Roukes 2001) (Ekinci 2005), like spin detection (Rugar et al. 2004) (Budakian, Mamin, and Rugar 2006), molecular mass detection (**Yang2006a**) (Jensen, Kim, and Zettl 2008) (Ilic et al. 2005), thermal fluctuation detection (Paul, Clark, and Cross 2006)

(Tamayo et al. 2007)(Snyder et al. 2007) (Badzey and Mohanty 2005), coupled resonance (Shim, Imboden, and Mohanty 2007)(Sato et al. 2003), biochemical reaction (Kwon et al. 2007) (Kwon et al. 2008) (Kwon et al. 2009) (Burg et al. 2007) (Campbell and Mutharasan 2006), etc.

Experiments have already been done fabricating and characterizing nanomechanical resonators, reaching UHF and VHF domains, upto GHz (Ekinci 2005) (Huang et al. 2005) (Peng et al. 2006). Significance variation in resonance and quality factor have been observed in the resonators at cryogenic temperatures (Husain et al. 2003). In our own lab, we studied the resonance and quality factor in a 5 micron long palladium beam with thickness 80 nm and width 200 nm at cryogenic temperature ($\sim$250 mK) as a function of temperature (**Indrajeet2014**).

The dissipation in nanomechanical resonators, described in detail in later sections, is due to sev-

eral extrinsic (surrounding, electronic circuit, etc.) and intrinsic (thermoelastic, lattice defects, etc.) factors (**Imbobden2013**). However, at cryogenic temperatures, thermal energy of the particles is much lower than the vibrational energy of the resonator (**Kunal2011**). So, impurities play a crucial role in dissipation at such cryogenic temperatures. In 1972, Phillips and Anderson (Phillips 1972) (Anderson, Halperin, and Varma 1972), simultaneously introduced a standard tunneling model in two level systems, to describe dissipation in amorphous solids due to presence of impurities. Though perfect crystals can't satisfy the required criterion for it to be implemented, but people have applied it to nano-scale devices, considering large surface to volume ratio pertaining to enough surface defects density such that the defects act like two level systems at sufficiently lower temperature, accounting for glassy behavior in crystalline solids autociteImboden2013.

In order to further modify the behavior of such systems, we want to introduce hydrogen to the palladium resonator at cryogenic temperatures. The hydrogen will get absorbed at the lattice sites of the palladium crystal, forming palladium hydride ($PdH_x, x \leq 1$) (Henriksson, Villanueva, and Brugger 2012a), and further increasing the impurity concentration in the lattice. In this way, we can further validate the applicability of the theory to the system. The absorption of hydrogen on the palladium lattice is reversible, which gives us considerable advantage in designing effective course of probing, as well as enabling us to probe multiple times without again changing the sample in dilution refrigerator, thus saving us a lot of time and effort.

1.1 Oscillators - SHM, Damped & Driven Damped

Oscillation generally refers to any type of periodic behaviour like pendulum, planetary motion, heart beat, etc. However, we will begin with the most common and simplest mechanical oscillation - the simple harmonic motions.

SHO A simple harmonic oscillator is defined as a system undergoing oscillations such that the restoring force on the body is directly proportional to the displacement of the body from the equilibrium point and is in the direction opposite to the velocity of the particle (French 1971).

Mathematically,

$$F = -kx \tag{1.1}$$

where, F = restoring force, x = displacement from equilibrium point and, k = proportionality constant depending upon the system.

In case of spring mass system, k is the spring constant, and the equation of motion of the system is given as:

$$m\ddot{x} + kx = 0 \tag{1.2}$$

where the mass m oscillates with angular frequency, $\omega_0 = \sqrt{\frac{k}{m}}$.

Damped Oscillation In case of damped motions, we introduce a resistance force term which is proportional to the velocity of the particle (**Gregory2006**),

$$R = -\beta v \tag{1.3}$$

and the equation of motion becomes:

$$F = -kx + R \implies m\ddot{x} + \beta\dot{x} + kx = 0 \tag{1.4}$$

where, β is a positive constant called resistance or damping constant.
The general solution to the system governed by above equation of motion is given by

$$x(t) = e^{\frac{-\beta t}{2}} \left(Ce^{\left(\omega_o \sqrt{\frac{\beta^2}{4\omega_o^2} - 1}\right) t} + De^{\left(-\omega_o \sqrt{\frac{\beta^2}{4\omega_o^2} - 1}\right) t} \right) \tag{1.5}$$

where, the term in parenthesis describes oscillation enveloped by an exponential decaying term.

Driven - Damped Oscillation In case of driven damped oscillation, we add an another term in the equation of motion, known as driving force which is a function of time (**Gregory2006**). In case of sinusoidal driving force with frequency ω,

$$G(t) = F_0 cos(\omega t), \tag{1.6}$$

so that the equation of motion becomes,

$$m\ddot{x} + \beta\dot{x} + kx = G(t) = F_0 cos(\omega t). \tag{1.7}$$

The steady state solution of the equation of motion described by above equation is given as,

$$x(t) = \frac{\frac{F}{m}}{\omega_o^2 - \omega^2 + i\frac{\omega\omega_o}{Q}}, \tag{1.8}$$

where the real and imaginary part of x descibes the 'In-phase' and 'Quadrature' amplitudes respectively.

1.2 Nano - Mechanical Resonators

Using Euler - Bernoulli equation for a doubly clamped beam of length L, width W and thickness T, the wave equation for oscillation in tha absence of any damping and external force is given as (**Cleland2004**):

$$EI\frac{\partial^4 z}{\partial x^4} - T_o\frac{\partial^2 z}{\partial x^2} + \rho A\frac{\partial^2 z}{\partial t^2} = 0 \tag{1.9}$$

where, E = Young's modulus of the material,

$I = \frac{WT^3}{12}$ = moment of inertia of the beam,

T_0 = intrinsic tension in the beam,

ρ = density of the material, and

A = cross-sectional area of the beam.

Now, imposing the boundary conditions for a doubly clamped beam (**Cleland2006**),

$$z(0,t) = z(L,t) = \frac{\partial z}{\partial x}(0,t) = \frac{\partial z}{\partial x}(L,t) = 0, \tag{1.10}$$

we get the expression for different frequencies of oscillation:

$$f_{on} = \frac{\pi}{8}(2n+1)^2\frac{1}{L^2}\sqrt{\frac{EI}{\rho A}}\sqrt{1+\frac{0.97T_oL^2}{(n+1)^2\pi^2 EI}}. \tag{1.11}$$

1.3 Dissipation

As we know, the term dissipation points towards the transformation of energy from one form to other, such that the capacity to do mechanical work in the later form is less than that in the former form. It is a result of an irreversible thermodynamic process in an inhomogenous environment. Several well known examples of dissipation are heat transfer, friction, etc.

Here we want to discuss various processes of dissipation in a nanomechanical resonator. In the given context, it can be described as the amount of energy lost per cycle of oscillation (Imboden and Mohanty 2013).

Though, a general description of dissipation in such systems are already present in literature, I would briefly state the common dissipation factors and only emphasize on dissipations of resonator caused by the presence of an external medium.

Extrinsic Dissipation As the name suggests, all external sources causing the dissipation in the system are termed as extrinsic dissipation sources. It includes dissipation caused due to improper device fabrication, due to measurements being carried out on the sample, effects of medium, temperature, etc.

Intrinsic Dissipation It includes all those dissipation sources which are consequences of the nature of material itself, like lattice defects in material, thermoelastic dissipation, etc.

Tunneling Two Level Systems (TTLS) At low temperatures, defects and impurities play a major role in dissipation. Standard tunneling model proposed by Anderson (Anderson, Halperin, and Varma 1972) and Phillips (Phillips 1972) (Phillips 1987) describes such behaviors of amorphos solids at low temperature using two level system.

According to the model, the defects occupy almost degenerate ground state, which can be compared to a double well potential model (Imboden and Mohanty 2013) with energy barrier much less than the available thermal energy, which forbids any thermal transition at temperatures much lower than 1K. Also, due to low temperatures, only two levels are considered, hence a double well potential model is approximated.

The TLS couple to the environment via strain, absorbing energy from the mechanical motion, thus modifying strain field and then releases the energy via resonant absorption. So, the TLS interacts with acoustic phonons, absorbing those of energy Δ and thus causes dissipation.

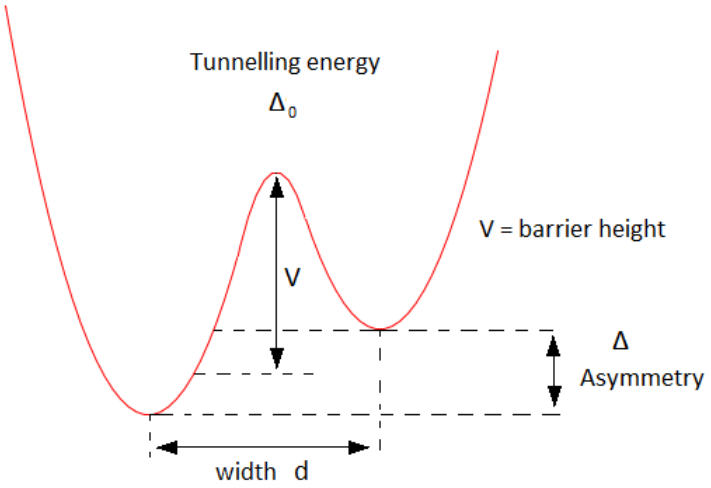

Figure 1.1: Two level system with double well potential model, adapted from (**Kunal2011**).

Another mechanism of dissipation in TLS is the relaxation absorption. In this case, the quantum tunneling between the two levels at higher frequency leads to dissipation via phonon pumping.

Dissipation due to medium As discussed by Mohanty (Imboden and Mohanty 2013), dissipation due to presence of medium around the resonator is analyzed in three regimes:

- The first one is the low pressure regime in which the concentration of molecules is so low that we take the limit of mean free path of the gas molecules greater than the dimension of resonator, such that there is no interaction between the gas molecules and the dissipation is due to momentum transfer between the oscillating beam and the gas molecules. Mathematically, it is given as (Newell 1968),

$$D_{LPD} = \left(\frac{2}{\pi}\right)^{2/3} \frac{1}{\rho t f_0} \frac{P}{v} \tag{1.12}$$

$$\approx 0.002 \frac{P}{\sqrt{E\rho}} \left(\frac{L}{t}\right)^2. \tag{1.13}$$

  where, P = pressure,

L = length of the beam,

t = beam thickness,

ρ = beam material density, and

E = Young's Modulus.

- As the pressure increases, we enter into the next one, which is viscous dissipation. In this case, due to the presence of a greater number of molecules, we get into continuum regime, such that the the resonator drags some of the medium along with it during oscillation, which increases the effective mass of the beam, resulting in dissipation.

  Mathematically,

$$D_{VD} \approx \frac{3.8\mu}{\sqrt{E\rho}w}\left(\frac{L}{t}\right)^2. \tag{1.14}$$

  where, w = beam width, and

  $\mu = 1.827 \times 10^{-7}$ Kg/(ms) is the viscosity of the medium.

- At still higher pressure, the gap between the resonator and the ground becomes filled with the medium, and the resonator has to squeeze the medium out from the gap to resonate. The respective damping is called squeeze film damping, mathematically given as:

$$D_{SFD} = \frac{\mu}{4\sqrt{E\rho}w}\left(\frac{L}{t}\right)^2\left(\frac{w}{g}\right)^3. \tag{1.15}$$

  where, g = gap between the beam and the substrate.

Frequency shift caused by hydrogen absorption The analysis of frequency shift caused by hydrogen absorption on the palladium beam is given by Henriksson.et.al. (Henriksson, Villanueva, and Brugger 2012a) in his electronic supplementary information: (Henriksson, Villanueva, and Brugger 2012b).

He assumed the resonant frequency of a clamped-clamped beam to be given as:

$$f_{res} \approx \frac{1}{2\pi}\sqrt{500\frac{<EI>}{<\rho A>}\frac{1}{L^4} + 12.3\frac{<\sigma A>}{<\rho A>}\frac{1}{L^2}}, \tag{1.16}$$

$$\approx \frac{1}{2\pi}\sqrt{42\frac{E_{Pd}}{\rho_{Pd}}\frac{t^2}{L^4} + 12.3\frac{\sigma}{\rho_{Pd}}\frac{1}{L^2}}, \tag{1.17}$$

where, $< EI >$ = beam bending stiffness,

$< \rho A >$ = mass per unit length, and

$< \sigma A >$ = longitudinal tensional force.

However, he says that the above equation is only valid when the second term in the square root is much smaller than the first one.

Next, on absorption of hydrogen into Pd, there are two different effects which he considered: increase in mass of the beam, and the volume expansion of the beam leading to compressive stress. Comparing the small H:Pd mass ratio, he neglects the effect of mass loading. Considering only the compressive stress, the relative shift in frequency is given by:

$$\frac{\Delta f}{f_{res}} \approx -0.1475 \frac{\sigma}{E} \left(\frac{L}{t}\right)^2 . \tag{1.18}$$

Dissipation due to hydrogen absorption at cryogenic temperatures We discussed earlier regarding the two level system which describes dissipation due to impurities in amorphous solids at low temperatures. But, it can not be applied directly to the crystalline nanoscale solids, though they have large surface to volume ratio resulting in considerable surface defects density.

The introduction of hydrogen to the system will lead to the formation of palladium hydride (PdH_x, x less than 1). The hydrogen thus getting at the lattice will develop compressive strain, and would further modify the biassed two level system, causing some new dissipation behavior.

The system can be compared to Zeeman splitting with certain analogies. In the case of Zeeman splitting, we have two degenerate states, up and down spins, before application of magnetic field. Applying the magnetic field creates biasness in the population among the two states. The strain developed in our case plays the similar role, creating biasness for pseudospins. This may modify the dissipation in the system at low temperature.

Chapter 2

Ultra Low Temperature Measurements

2.1 Introduction

Ultra low temperature, or cryogenic temperature generally refers to temperatures below what is generally reached by common refrigerants like Freons, hydrogen sufide, etc. Though there is no fine line as such, the National Institute of Standards and Technology at Boulder, Colorado has chosen 93.15K as the limiting temperature.

2.2 Why Low Temperature Measurements?

To answer the question, first we have to understand the physical significance of two fundamental constants used regularly in physics: Planck's constant, h (also used sometimes reduced Planck's constant or Dirac constant, $\hbar$) and Boltzmann constant, k_T.

Planck's constant is defined as the quantum of action in quantum mechanics. It describes the quantization of light and matter.

In SI units,

$$h = 6.626 \times 10^{-34} Js \qquad and, \qquad \hbar = \frac{h}{2\pi} = 1.054 \times 10^{-34} Js. \tag{2.1}$$

The smallness of the value of Planck's constant indicates the presence of immense number of infinitesimal quantized particles. For example, considering light of any visible frequency, Planck's constant times its frequency gives the energy of each quantized photon, which is so small that we would need million such photons to see them.

Next is the Boltzmann's constant. It relates the energy of a particle due to its absolute temperature, or thermal energy to the kinetic energy. With the help of ideal gas law, it also bridges the gap between microscopic and macroscopic world.

In SI units,

$$k_B = 1.38 \times 10^{-23} JK^{-1}. \tag{2.2}$$

Now, since we are familiar with both constants, $\hbar\omega$ is the vibrational energy of the system, while $k_B T$ is the thermal enrgy of the system. At normal room temperatures, thermal energies are quite greater than vibrational energy, which suppresses the quantum effects from being observed in most cases. However, at lower temperatures,

$$\hbar\omega \geq k_B T, \tag{2.3}$$

thus, we expect to observe some quantum phenomenons at lower temperatures. This is the reason behind taking the sample to such low temperatures.

Also, only low temperature is not sufficient. We also need high ω, which requires miniaturisation of the oscillator, since resonant frequency is inversely proportional to L^2 (Eom et al. 2011).

2.3 Dilution Refrigerator

Dilution refrigerator is a cryogenic device using which we get into ultra low temperature regime upto mK range. It was first proposed by Heinz London in the early 1950s. However, it was realized experimentally in 1964 in the Kamerlingh Onnes Laboratorium at Leiden University.

It is not possible to reach temperatures far below 1 K using regular refrigeration techniques. However, dilution refrigerator allows us to reach mK temperatures under continuous operation. It uses a very unique property of liquid ^{3}He/^{4}He mixture to reach such low temperatures, which we are going to discuss soon.

2.3.1 Properties of Liquid ^{3}He/^{4}He Mixture

To understand the working of a dilution refrigerator, first we need to get familiar with some of the basic properties of liquid ^{3}He/^{4}He mixture. Figure 2.1 shows the phase separation of liquid ^{3}He/^{4}He mixture in the phase diagram as we decrease the temperature.

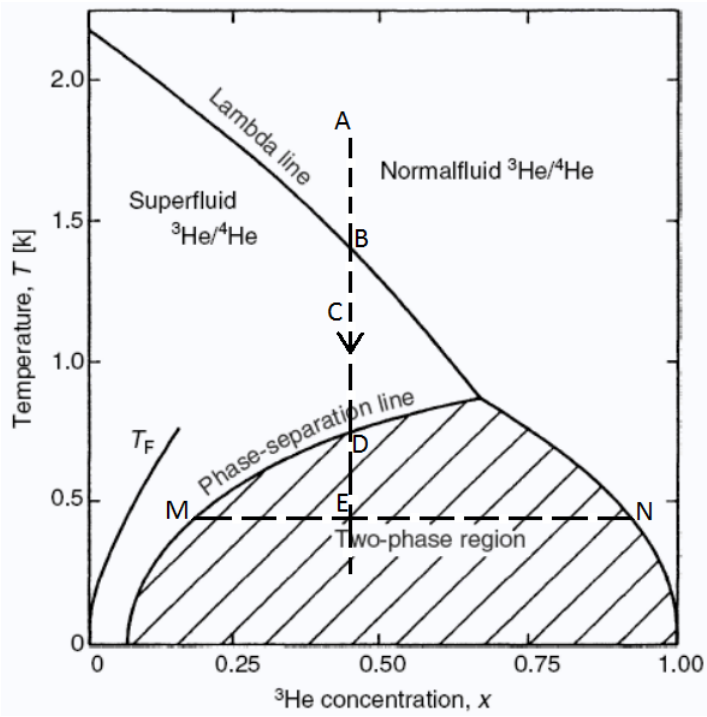

Figure 2.1: Phase diagram for liquid He3-He4 mixture (**Hock2009**).

As Hock described using the phase diagram (**Hock2009**), the x-axis is the fraction of ^{3}He in the liquid ^{3}He/^{4}He mixture and y-axis is the temperature (in Kelvin).

Now, if we take some liquid ^{3}He/^{4}He mixture begining at point A from the phase diagram and gradually decrease the temperature to point E. As evident from the phase diagram, initially both liquids are normal liquids (non-superfluid liquids). When the mixture reaches point B in the phase diagram, it crosses the lambda line, and ^{4}He becomes superfluid liquid, with ^{3}He remaining as it was earlier, and we get into region C.

When the temperature is further reduced, the mixture reaches point D on the phase separation line, which separates the mixture into two phases, one rich in ^{3}He and the other rich in ^{4}He. So, the shaded region is the forbidden region *i.e.* the mixture can't have the temperature and concentration of that denoted in the shaded region. So, for a temperature corresponding to that in the shaded region, like point E, it is only possible to have a mixture with concentration of ^{3}He below pont M or above point N. For the present case, we will get two separate mixtures, one having concentration at M, and the other having concentration at N (**Hock2009**) (**Betts1989**).

Mixture at point M, having higher concentration of ^{3}He is called concentrated phase, and that at point N, having lower concentration of ^{3}He is known as dilute phase. Also, ^{3}He being less dense, the concentrated phase floats on the dilute phase.

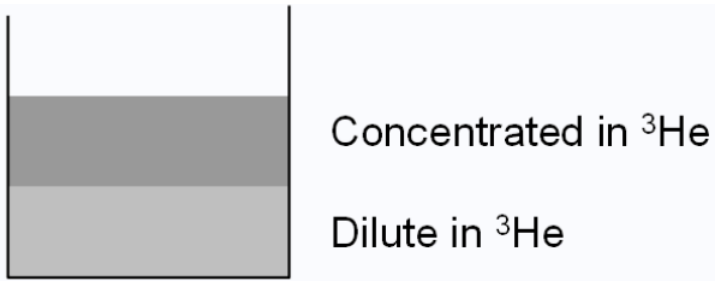

Figure 2.2: Phase separation of concentrated and dilute phase (**Hock2009**).

2.3.2 Cooling by Dilution

In the above section, we came to know about a very interesting property of liquid ^{3}He/^{4}He mixture, *i.e*. phase separation at lower temperatures.

However, we didn't discussed its significance in providing cooling. The cooling power comes from the fact that the enthalpy of mixing of liquid ^{3}He into liquid ^{4}He is positive, means the process is endothermic. So, we pump out the ^{3}He from the dilute phase, decreasing ^{3}He concentration in the dilute phase, which pulls ^{3}He from the concentrated phase into dilute phase and extracts heat from the surrounding in this process of mixing ^{3}He into ^{4}He.

Hock compared the process to evaporation (**Hock2009**). In evaporation, cooling takes place when atoms move from liquid to vapour phase. Similarly, in dilution cooling, atoms of ^{3}He move from concentrated to dilute phase.

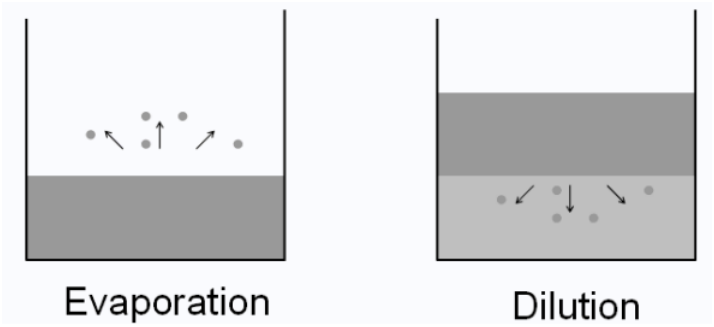

Figure 2.3: Analogy between evaporation and dilution cooling (**Hock2009**).

As seen from the phase separation diagram, in which the graph becomes almost vertical as temperature tends to absolute zero, indicating no concentration variation in dilute phase at even lower temperatures. This ensures the applicability of the process at even lower temperatures. While in the case of evaporative cooling (say of liquid helium), vapour pressure decreases with decreasing temperature, decreasing further vapourisation and limiting further cooling.

2.4 Experiments in Dilution Refrigerator

As a part of his final year masters project work, Indrajeet characterized an approximately 5 micron long beam of width 200 nm and thickness 80 nm, studying the shift in resonance and dissipation with variation in temperature from 170 mK to 1 K. A SEM image of the measured sample is shown.

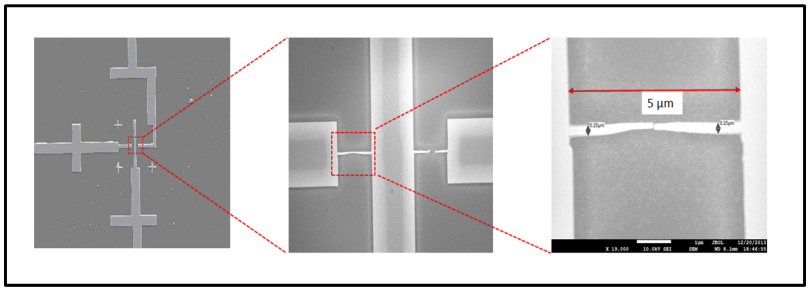

Figure 2.4: SEM image of the measured sample.

At room temperature, the resonance was observed at 33.8 MHz. VNA R&S ZVB14 was used for RF measurements. The complete resonance peak with real and imaginary components plotted at room temperature along with the shift in resonance with varying temperature is shown.

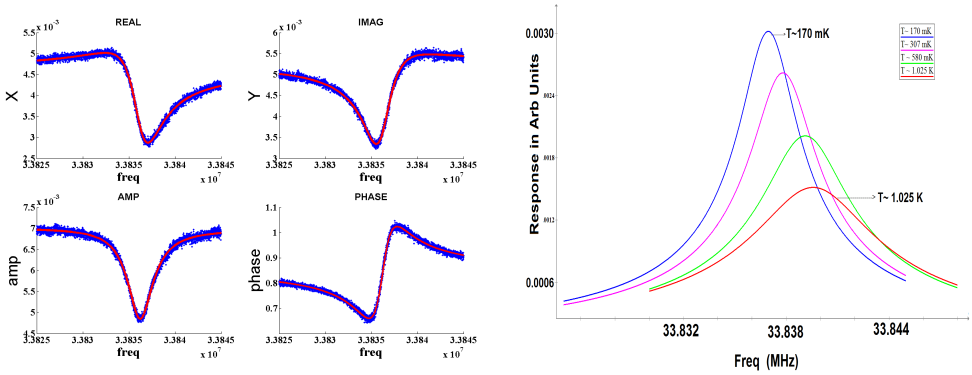

Figure 2.5: Left: Resonance at room temperature, and Right: Shift in resonance at cryogenic temperatures.

The dilution refrigerator used for reaching cryogenic temperature was TRITON 200, manufactured by Oxford Instruments. A detailed diagram with all the components is shown in the next figure, along with an actual photograph of the instrument in our lab. The cold finger, where sample was kept, is enlarged for clarity. Near the cold finger, wirings for the super-conducting magnet could be seen, which gives magnetic field upto 9 T, which enabled us to carry out measurements using magnetomotive technique.

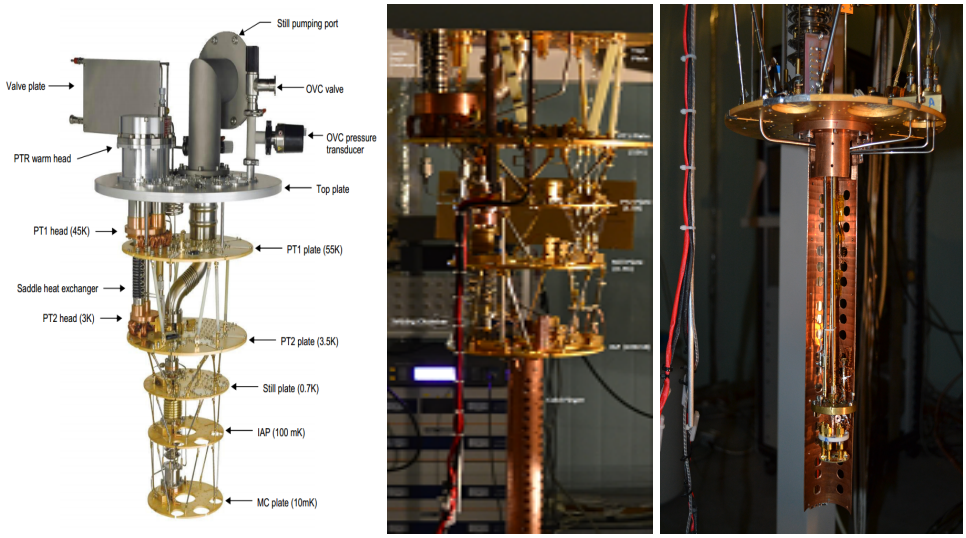

Figure 2.6: Left: Components of Cryofree Dilution Refrigerator TRITON 200 from Oxford Instruments Manual, Middle: Same model in our lab, and Right: Cold finger with the sample before starting cool down.

Though the resonance peak and its shift on varying temperature in cryogenic range was obtained, nothing could be done to change physical properties of the sample itself, to study any other effect.

However, if we could anyhow introduce hydrogen gas to the palladium sample, it would absorb some of the hydrogen into its lattice, which increases the mass of the resonating beam and introduces a compressive strain in the beam. These changes in the beam are expected to further change the properties like resonance and quality factor of the beam.

Thermal and acoustoic properties of bulk solids are well understood in terms of models based on tunelling two level systems (TLS) The dissipation in a nano-scale resonators at low temperature is described using standard tunelling model in two level system as reviewed by(**Imbobden2013**). Although key features of the TLS are displayed by nanoscale devices an exact theoretical picture is not available.

There is also not good experimental data on many materials. We want to understand simple metallic resonators. Palladium was chosen as hydrogen will change its mechanical and electrical properties. So, introduction of hydrogen into palladium lattice would give us another tool to probe at different scenarios of TLS with same device.

But, the problem is the introduction of hydrogen to the palladium sample. Inside the fridge, there is a single vacuum space where all the different stages are maintained at different temperatures, as apparent in fig. 2.6. To reach millikelvins in the refrigerator, we have to pump out that space upto a vacuum of order $10^{-3} - 10^{-4}$ mtorr and even lower, to prevent heating up of sample through convection. Filling up with hydrogen will lead to condensation of hydrogen at the wall, thus cooling outer wall. So, it won't provide effective cooling of the system and sample space.

Also, if we once fill the cold chamber with hydrogen, it will condense into the super insulating

shielding unit of layers of Mylar and fiber fillings, and would give fake hydrogen leak in the future. Flammability of hydrogen is another problem.

So, we need a chamber with an input gas line which can be placed inside the cold finger and accommodate the sample. It could solve the problems mentioned above, as it would not fill the whole cryostat thus not interrupting the cooling process of the system. Introducing small volume of hydrogen also eliminates the danger of flammability of hydrogen. But the chamber should be vacuum tight and leak proof even at cryogenic temperature, otherwise we will again get the same problem.

We have to also take care of the electrical wirings so as to read the sample. So, we needed both DC and radiofrequency connections through the chamber which would remain leak proof at cryogenic temperatures. The main challange that we come through while designing the required can is getting hermetic RF feedthrough which should work at cryogenic temperatures.

For the given sample, we needed three radiofrequency connections, two DC connections and one gas line going inside the vacuum chamber to the sample, all leak proof at cryogenic temperatures. For DC wiring, we chose twisted pairs. RF signals required SMAs: two of them for input and one for output.

As shown in the SEM image of the sample (fig. 2.7), two SMAs as input are needed to be connected to the left and right pads, giving input at 180^0 phase to each other and one output to the middle strip, so that any stray capacitances like connections to the sample will effectively cancel out (Ekinci 2005).

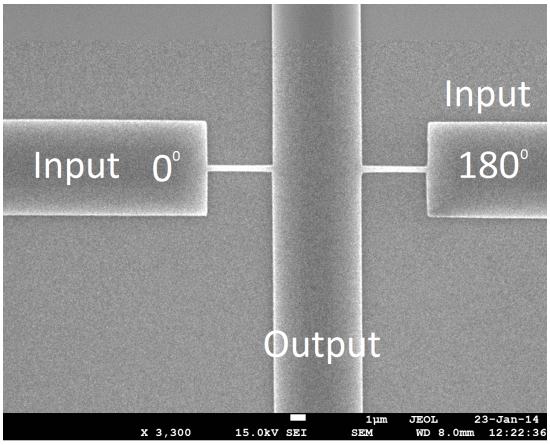

Figure 2.7: Balanced bridge measurement scheme.

In the upcoming chapter, the whole course of designing hermetic DC and RF feedthroughs for using vacuum can inside the cryostat at cryogenic temperatures is discussed in detail.

Chapter 3

Cryogenic Hermetic DC and RF feed-throughs

As discussed earlier, to do the required modification with the sysytem by introducing hydrogen, we need a vacuum chamber. It should be small enough to be accommodated in the space available between the magnets, inside the cold finger, as well as equipped with three SMAs, DC wirings and a gas supply or vacuum line. All the feedthroughs should be hermetic at cryogenic temperatures.

For choosing the suitable material for the body of the can, we compared several materials. Brass had closer coefficent of thermal expansion as stycast, when compared to copper. Also, it is easily machinable.

Indium is standardly used to make cryogenic vacuum seals (**Richardson1998**). It is a very malleable metal, and so is easily crushed on applying pressure. However, since it is a metal, it does not crack, as rubber does, at low temperatures. It is capable of undergoing many cycles of heating and cooling without cracking.

In the upcoming figure, a cross section schematic of the assembly is presented to give a simple idea of how the lid was sealed to the can using indium wire. After placing the indium wire in the gap, the screws were tightened, thus crushing the indium wire to form uniform cryogenic seal. While placing the wire, it was crossed after covering the circumference of the can, so that the end could merge with each other, giving proper seal. Other components like vacuum/gas supply and DC wiring brass tube are also illustrated.

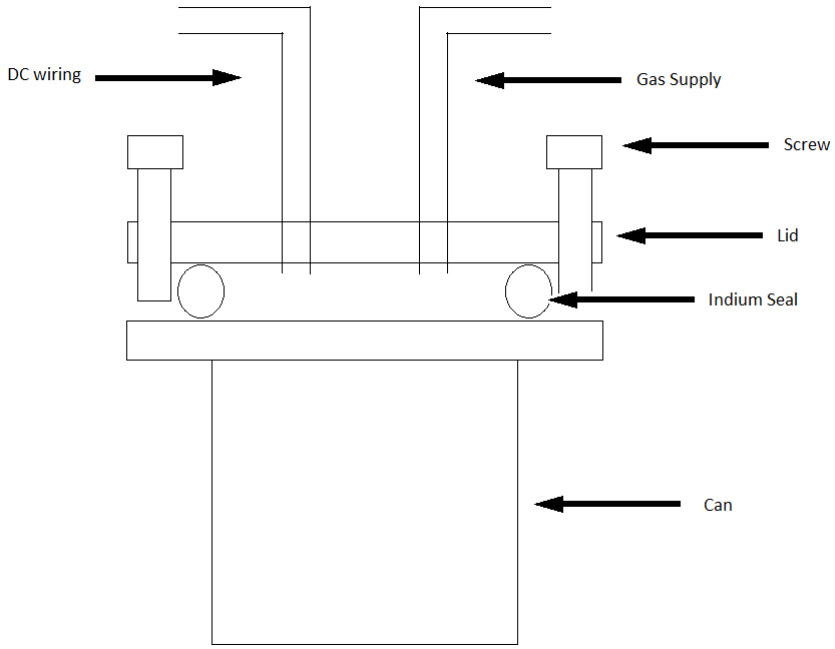

Figure 3.1: Schematic drawing of indium seal between the can and the lid..

3.1 Vacuum Tight Fittings

For vacuum/gas supply shown in the schematic, stainless steel tube was used.

Since one end will be outside the cryostat with KF-25 connection at room temperature, it should also be a poor thermal conductor to minimize the heat load. Stainless steel is both a poor thermal conductor and a rigid material.

In the beginning, we used quarter inch SS tube, but later changed into one-eighth inch one. Stainless steel thus satisfy the purpose.

Though the can is shown to be sealed using the indium wire seal in the schematic (fig 3.2), all other fittings like vacuum/gas supply, DC and RF feedthroughs, etc. should also have vacuum integrity, which is checked using Helium leak detector. In Helium leak detector, the required system to be checked is connected to the detector using a KF-25 port. After calibrating the mass spectrometer with a calibrated leak inside the system, it starts pumping on the available space (volume of can in our case), creating vacuum of the order 10^{-3} mbar.

To check for leaks, helium gas is sprayed at the joint fittings and other potential areas which are susceptible to leak. In case of a leak present in the system, the helium atoms seeps inside and reaches the leak detector, where it gets detected by mass spectrometer. There is a dedicated pump for the mass spectrometer which prevents the mass spectrometer from being saturated with helium. The leak detector produces an audible alarm when the leak rate is greater than 10^{-9} mbar.l/s.

Figure 3.2: Helium leak detector.

Though 10^{-8} mbar l/s is acceptable leak rate, we aimed for 10^{-9} mbar l/s to be on the safe side against condensation which might be caused by leaking.

In the schematic diagram (fig 3.2), as the screws are tightened, the indium wire gets crushed, forming a nice seal. However, the tubes for gas supply as well as DC wiring should also be sealed properly.

In the begining, we tried soldering to join the tubes with the lid. Brass tube could be soldered nicely. A photograph of the brass tube soldered to the lid is shown in fig. 3.3.

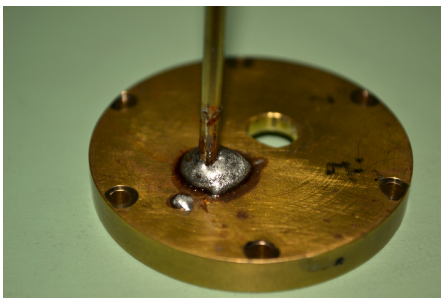

Figure 3.3: Brass tube soldered to brass lid.

But solder doesn't stick to steel, giving leaks. So, we tried brazing next. Brazing is done at a little higher temperature (around 700^0 C) as compared to soldering which is done at around 400^0 C. We have to ensure beforehand that all the materials are red hot before applying flux and brazing rod

(brass or copper) in brazing.

Figure 3.4: Both brass tube and SS tube brazed to brass lid.

Thin brass tube should not be heated too much as it, after becoming red hot, melts, creating holes which could leak. Since thin brass tube worked fine with soldering, we first brazed the SS tube and then soldered the thin brass tubes to the lid. Soldering should not be done before doing brazing as doing brazing afterwards will melt the solder.

Though brazing worked, it was not a 100% assurance, as even nice brazing works leaked sometimes. Stycast is known to give leak tight sealing at cryogenic temperatures, as it flow into the gaps and becomes rock hard. So, we tried stycast over brazed sections to prevent further leaks, which finally worked. We even covered the soldered brass tube joint with stycast to further ensure leak tight fitting.

Figure 3.5: SS tube, first brazed, and then covered with stycast to the KF-25 blank, used to connect can with bellow, while testing leak using helium leak detector.

Before using stycast, one must be aware of all the precautionary measures. Gloves should be used to handle the resin as well as hardener, and direct skin contact should be avoided. Goggles should be used for eye protection. Vapors from the catalyst should also be avoided from inhaling, as it may cause some irritations in the respiratory system.

Both the resin and hardener should be weighed properly in a clean container in the recommended ratio. In our case, we used catalyst 23 LV, which is required 7.5% as the weight of the

resin. Both the components should be mixed using a kneading motion for 2-3 minutes to produce an uniform mixture. To ensure that no air is entrapped in the mixture, vacuum dearing should be used at 1-5 mm mercury for 3-10 minutes till most of the bubbling has ceased. The whole process should be done inside fumehood to avoid inhaling vapors. After vacuum dearing, the mixture should be applied at the required cavity or surface and should be allowed to cure for the required schedule (24 hrs at 25^0C in our case). The region to be applied should be cleaned properly before application to remove any contaminant like dust, moisture, oils etc. which can cause corrosion or poor adhesion.

Once all the connections to the lid are assured to be leakproof, we need to place the can inside the cold finger in dilution refrigerator. But the SS tube going to supply gas to the sample won't be staright and single piece. Instead, there would be many small pieces which wil be bent and joined in between.

Since swagelok fittings are routinely used at liquid nitrogen temperatures, we expest them to work. The ferrules of the swagelok fitting deforms the metal at the joint and thus give proper leak proof connection.

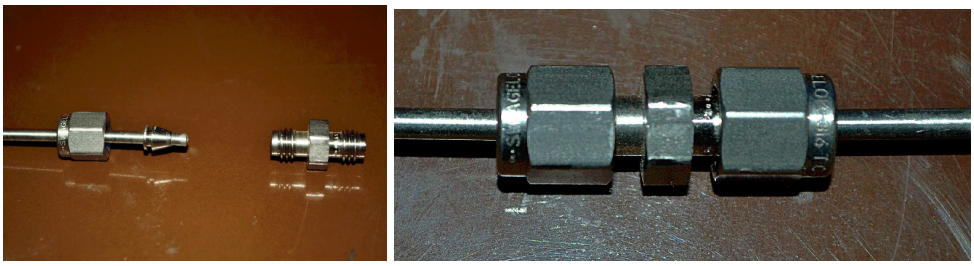

Figure 3.6: Left: Components of swagelok tube and the alignment for application, Right: Two SS tubes joined using swagelok fitting.

3.2 Hermetic DC feed-through

For hermetic DC feedthrough, we used the general procedure of filling thin brass tube carrying twisted pair with stycast. First we made a leakproof thin brass tubing on the lid through wich we inserted the twisted pairs and finally sealed it filling the whole tube with stycast. Thin brass tube was used to minimize the heat load on the cryostat. For joint leakage, soldering was used covered with stycast, as described in previous section.

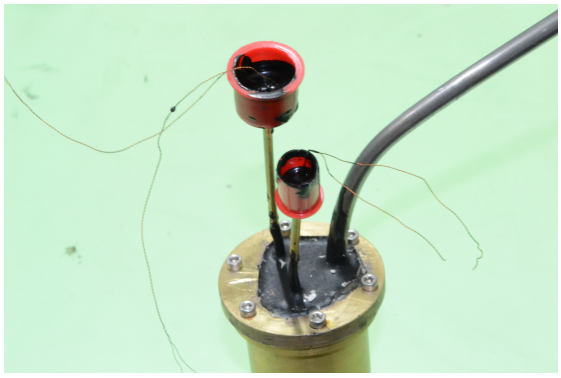

Figure 3.7: Twisted pair passing through brass tube into the can, sealed with stycast filled into the brass tube. SS tube is seen in the right for checking vacuum, further supposed to be the gas supply.

3.3 Hermetic RF feed-through

The main challange in designing the whole can was getting RF feedthrough. The SMA connectors we generally use at room temperatures are filled with teflon. So, even if we make them leakproof at lid using stycast, the cable will leak.

Though there are some weldable SMAs with ceramic dielectric joints in the market which can serve the purpose, they are expensive and bulky. Even if we get one of them, getting other feedthroughs in the same space will be a problem. Also, it would require that all feedthroughs are welded in one go.

One way through this was using the commercially available glass bead connectors, which could be sealed using solder to give hermetic seal. They are used for connecting to PCBs, and have 50 Ω resistance. However, in this case, it would need SMAs on both sides.

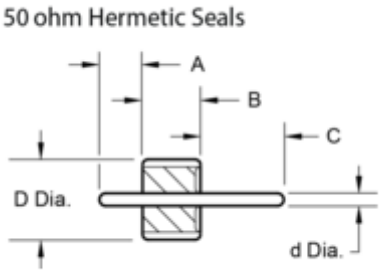

Figure 3.8: Glass bead which is soldered inside SMA. Image taken from Southwest Microwave catalog.

As a novel solution to this problem, we decided to use commercial vacuum tight SMA feedthroughs for room temperature application. These feedthroughs have a glass bead soldered in between to adapters as shown in the schematic in figure 3.9.

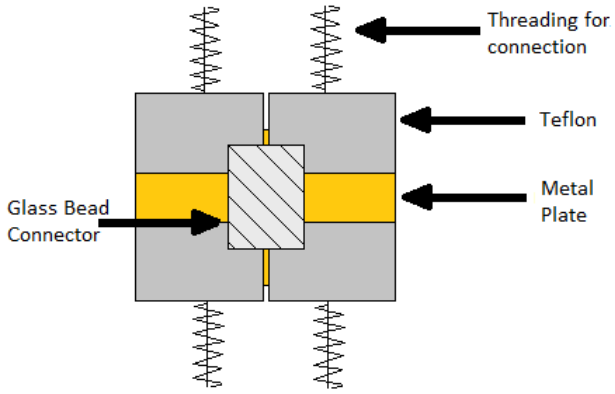

Figure 3.9: Schematic of SMA from Huber-Suhner.

SMA cables can be connected to both ends of the adapter. On a metal plate, an additional flange to accommodate a rubber O-ring is provided. The rubber O-ring makes sure there is no leak between the flange and the metal plate. The glass bead ensures that there can be no leak through the teflon dielectric at both ends.

A picture of the connector is shown in 3.10 (Left).

Our simple and yet effective solution was to replace the rubber O-ring with an indium wire. This must ensure that we get a leak tight as well as good 50 Ω matched RF connector.

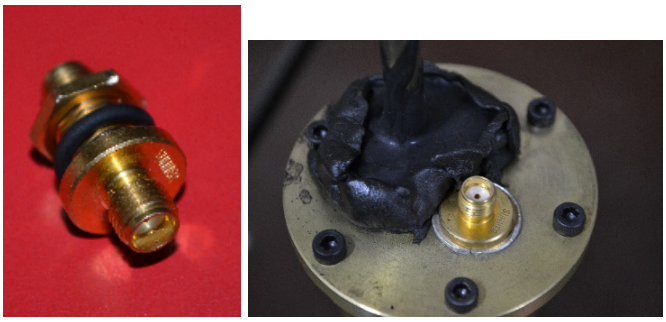

Figure 3.10: Left:SMA jack to jack connector from Huber-Suhner, Right: Rubber O-ring replaced with Indium O-ring while testing.

3.4 Final Can Design

Finally, after testing each components separately, we finally got assured of all the working electrical and gas tubing connections. Then we first designed the can and lid using solidworks, estimating and optimizing the design as per available space between the magnets in the dilution refrigerator.

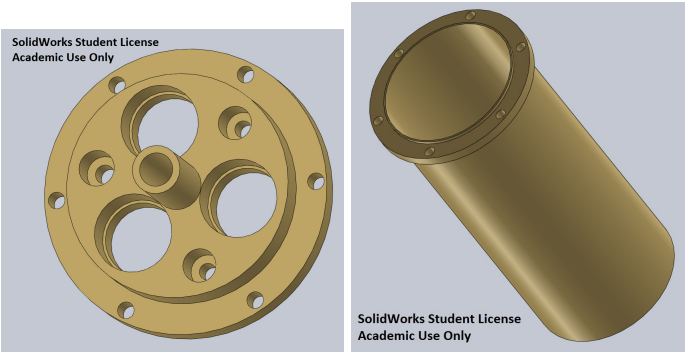

Figure 3.11: Left: Lid of the can with space for three SMAs, two DC and one gas connection, Right: Can to accommodate the sample.

Figure 3.11 shows the design. Groves were made to accommodate the SMA adapter. As the thickness of the plate can not be very high to thread in the connector properly. The thicker portion were used to have small holes to braze or solder metal tube. This ensures long enough portion was brazed/soldered properly. The holes for the tube also had small countersinks to pour the stycast.

After brazing the tubes the indium seal for the RF connection were done. Finally the indium seal for the can was done to check the whole system for vacuum integrity. The system typically showed leak rates of the order of 10^{-9} mbar.l/s. A similar leak rate was also observed when the system was dipped in liquid nitrogen.

And finally we machined the actual pieces from brass, using lathe and drilling machines.

Figure 3.12: Actual can with three SMAs, two DC and one gas connection.

It was tested to be working perfectly when plunged into liquid nitrogen. Most materials don't contract much below 77 K. So, if it is working at liquid nitrogen temperature, it should also work at cryogenic temperatures.

3.5 Indium Wire Extruder

As we have seen earlier, Indium is used both for sealing gaps between can and lid, and for RF connection using SMA.

For sealing between can and lid, around 165 mm long Indium wire of diameter 0.7 mm is used during every testing (of gas tubing, DC wiring, etc.). For RF testing, an additional 2 mm diameter Indium wire of length 25 mm is used.

So, taking into account of the cost, we designed an Indium wire extruder to recycle the used Indium.

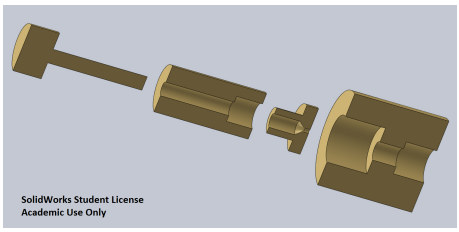

Figure 3.13: Cross section.of Solidworks drawing of Indium extruder. Four components are: piston, chamber, shaping die and holder (from top to bottom).

As clear from the name itself, we fill the chamber with used scrapes of Indium, with suitable shaping die in front. Then we insert the piston and place the whole assembly consisting of holder in the bottom beneath the hydraulic press. On applying the pressure, we get the Indium wire of desired diameter, using suitable shaping dye.

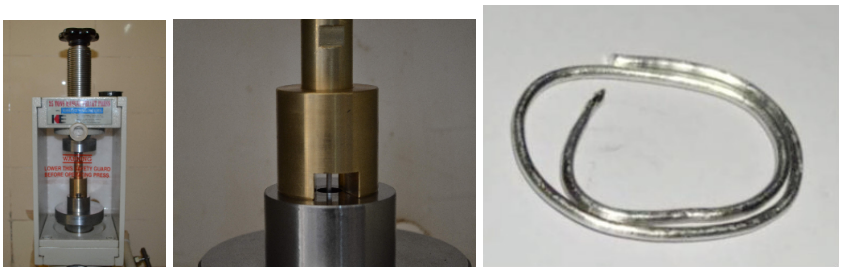

Figure 3.14: Left: Indium wire extruder placed beneath hydraulic press, Middle: Close-up of extruder in action showing extruded Indium wire from below and Right: Final extruded Indium wire.

Conclusion

Experimental trials comprising the fabrication of required hermetic feedthroughs via vacuum can to be used at cryogenic temperatures is presented in this work. Stycast proved to be a preferable hermetic sealant capable of working at cryogenic temperatures. But it should be applied only after the pieces are brazed carefully. For RF feedthrough, we were struggling at the beginning. However, we found the room temperature hermetic SMA and replacing its rubber O-ring with indium O-ring proved to be the optimum solution of the problem.

All the working components were tested using helium leak detector, first at room temperature, and then at liquid nitrogen temperature. While testing for liquid nitrogen temperature, the whole volume of can was dipped inside the liquid nitrogen, thus abruptly lowering the temperature of the can, and delivering cold shocks.

So, getting leak tight working connections on shocking the components assures that they will work inside the dilution refrigerators also, since the cooling inside the dilution refrigerator is much gentler and smoother.

Finally, with all the components found working even after all combined, we hope to perform the long waited experiment without any further obstacles.

Bibliography

Anderson, P. w., B. I. Halperin, and c. M. Varma (Jan. 1972). "Anomalous low-temperature thermal properties of glasses and spin glasses". In: *Philosophical Magazine* 25.1, pp. 1–9. ISSN: 0031-8086. DOI: 10.1080/14786437208229210. URL: http://dx.doi.org/10.1080/14786437208229210.

Badzey, Robert L and Pritiraj Mohanty (Oct. 2005). "Coherent signal amplification in bistable nanomechanical oscillators by stochastic resonance." In: *Nature* 437.7061, pp. 995–8. ISSN: 1476-4687. DOI: 10.1038/nature04124. URL: http://dx.doi.org/10.1038/nature04124.

Budakian, R., H. J. Mamin, and D. Rugar (Sept. 2006). "Spin manipulation using fast cantilever phase reversals". In: *Applied Physics Letters* 89.11, p. 113113. ISSN: 00036951. DOI: 10.1063/1.2349311. URL: http://scitation.aip.org/content/aip/journal/apl/89/11/10.1063/1.2349311.

Burg, Thomas P et al. (Apr. 2007). "Weighing of biomolecules, single cells and single nanoparticles in fluid." In: *Nature* 446.7139, pp. 1066–9. ISSN: 1476-4687. DOI: 10.1038/nature05741. URL: http://dx.doi.org/10.1038/nature05741.

Campbell, Gossett A and Raj Mutharasan (Apr. 2006). "Use of piezoelectric-excited millimeter-sized cantilever sensors to measure albumin interaction with self-assembled monolayers of alkanethiols having different functional headgroups." In: *Analytical chemistry* 78.7, pp. 2328–34. ISSN: 0003-2700. DOI: 10.1021/ac0517491. URL: http://dx.doi.org/10.1021/ac0517491.

Ekinci, K. L. (2005). *Electromechanical Transducers at the Nanoscale: Actuation and Sensing of Motion in Nanoelectromechanical Systems (NEMS) - ekinci review.pdf*. URL: http://nanoscience.bu.edu/papers/ekincireview.pdf.

Eom, Kilho et al. (June 2011). "Nanomechanical resonators and their applications in biological/chemical detection: Nanomechanics principles". In: *Physics Reports* 503.4-5, pp. 115–163. ISSN: 03701573. DOI: 10.1016/j.physrep.2011.03.002. arXiv:1105.1785. URL: http://arxiv.org/abs/1105.1785.

French, AP (1971). *Vibrations and Waves*. W . W . NORTON & COMPANY. INC. NEW YORK, pp. 62–68. DOI: 10.1007/SpringerReference_63.

Henriksson, Jonas, Luis Guillermo Villanueva, and Juergen Brugger (Aug. 2012a). "Ultra-low power hydrogen sensing based on a palladium-coated nanomechanical beam resonator." In: *Nanoscale* 4.16, pp. 5059–64. ISSN: 2040-3372. DOI: 10.1039/c2nr30639e. URL: http://www.ncbi.nlm.nih.gov/pubmed/22767251.

— (Aug. 2012b). "Ultra-low power hydrogen sensing based on a palladium-coated nanomechanical beam resonator." en. In: *Nanoscale* 4.16, pp. 5059–64. ISSN: 2040-3372. DOI: 10.1039/c2nr30639e. URL: http://pubs.rsc.org/en/content/articlehtml/2012/nr/c2nr30639e.

Huang, X M H et al. (Nov. 2005). "VHF, UHF and microwave frequency nanomechanical resonators". en. In: *New Journal of Physics* 7.1, pp. 247–247. ISSN: 1367-2630. DOI: 10.1088/1367-2630/7/1/247. URL: http://iopscience.iop.org/1367-2630/7/1/247/fulltext/.

Husain, A. et al. (Aug. 2003). "Nanowire-based very-high-frequency electromechanical resonator". In: *Applied Physics Letters* 83.6, p. 1240. ISSN: 00036951. DOI: 10.1063/1.1601311. URL: http://scitation.aip.org/content/aip/journal/apl/83/6/10.1063/1.1601311.

Ilic, B et al. (May 2005). "Enumeration of DNA molecules bound to a nanomechanical oscillator." In: *Nano letters* 5.5, pp. 925–9. ISSN: 1530-6984. DOI: 10.1021/nl050456k. URL: http://dx.doi.org/10.1021/nl050456k.

Imboden, Matthias and Pritiraj Mohanty (2013). "Dissipation in nanoelectromechanical systems". In: *Physics Reports*. URL: http://www.sciencedirect.com/science/article/pii/S0370157313003475.

Jensen, K, Kwanpyo Kim, and A Zettl (Sept. 2008). "An atomic-resolution nanomechanical mass sensor." en. In: *Nature nanotechnology* 3.9, pp. 533–7. ISSN: 1748-3395. DOI: 10.1038/nnano.2008.200. URL: http://www.nature.com/nnano/journal/v3/n9/abs/nnano.2008.200.html.

Kwon, Tae Yun et al. (June 2007). "In situ real-time monitoring of biomolecular interactions based on resonating microcantilevers immersed in a viscous fluid". In: *Applied Physics Letters* 90.22, p. 223903. ISSN: 00036951. DOI: 10.1063/1.2741053. URL: http://scitation.aip.org/content/aip/journal/apl/90/22/10.1063/1.2741053.

Kwon, Taeyun et al. (Oct. 2008). "Micromechanical observation of the kinetics of biomolecular interactions". In: *Applied Physics Letters* 93.17, p. 173901. ISSN: 00036951. DOI: 10.1063/1.3006329. URL: http://scitation.aip.org/content/aip/journal/apl/93/17/10.1063/1.3006329.

Kwon, Taeyun et al. (Jan. 2009). "Nanomechanical in situ monitoring of proteolysis of peptide by Cathepsin B." In: *PloS one* 4.7, e6248. ISSN: 1932-6203. DOI: 10.1371/journal.pone.0006248. URL: http://www.plosone.org/article/info:doi/10.1371/journal.pone.0006248;jsessionid=C39D9EA9AE2B1BBBFB50FB91C08F9F8D.

Newell, W E (Sept. 1968). “Miniaturization of tuning forks.” In: *Science (New York, N.Y.)* 161.3848, pp. 1320–6. ISSN: 0036-8075. DOI: 10.1126/science.161.3848.1320. URL: http://www.ncbi.nlm.nih.gov/pubmed/17831341.

Paul, M R, M T Clark, and M C Cross (Sept. 2006). “The stochastic dynamics of micron and nanoscale elastic cantilevers in fluid: fluctuations from dissipation”. In: *Nanotechnology* 17.17, pp. 4502–4513. ISSN: 0957-4484. DOI: 10.1088/0957-4484/17/17/037. URL: http://stacks.iop.org/0957-4484/17/i=17/a=037.

Peng, H. et al. (Aug. 2006). “Ultrahigh Frequency Nanotube Resonators”. In: *Physical Review Letters* 97.8, p. 087203. ISSN: 0031-9007. DOI: 10.1103/PhysRevLett.97.087203. URL: http://link.aps.org/doi/10.1103/PhysRevLett.97.087203.

Phillips, W. A. (May 1972). “Tunneling states in amorphous solids”. In: *Journal of Low Temperature Physics* 7.3-4, pp. 351–360. ISSN: 0022-2291. DOI: 10.1007/BF00660072. URL: http://link.springer.com/10.1007/BF00660072.

Phillips, W A (Dec. 1987). “Two-level states in glasses”. en. In: *Reports on Progress in Physics* 50.12, pp. 1657–1708. ISSN: 0034-4885. DOI: 10.1088/0034-4885/50/12/003. URL: http://iopscience.iop.org/0034-4885/50/12/003.

Roukes, M.L. (2001). *Nanoelectromechanical systems face the future*. DOI: 2001. URL: http://nano.caltech.edu/publications/papers/phyworld.pdf.

Rugar, D et al. (July 2004). “Single spin detection by magnetic resonance force microscopy.” In: *Nature* 430.6997, pp. 329–32. ISSN: 1476-4687. DOI: 10.1038/nature02658. URL: http://dx.doi.org/10.1038/nature02658.

Sato, M. et al. (Jan. 2003). “Observation of Locked Intrinsic Localized Vibrational Modes in a Micromechanical Oscillator Array”. In: *Physical Review Letters* 90.4, p. 044102. ISSN: 0031-9007. DOI: 10.1103/PhysRevLett.90.044102. URL: http://link.aps.org/doi/10.1103/PhysRevLett.90.044102.

Shim, Seung-Bo, Matthias Imboden, and Pritiraj Mohanty (Apr. 2007). “Synchronized oscillation in coupled nanomechanical oscillators.” In: *Science (New York, N.Y.)* 316.5821, pp. 95–9. ISSN: 1095-9203. DOI: 10.1126/science.1137307. URL: http://www.sciencemag.org/content/316/5821/95.abstract.

Snyder, Phillip W et al. (Feb. 2007). “A stochastic, cantilever approach to the evaluation of solution phase thermodynamic quantities.” In: *Proceedings of the National Academy of Sciences of the United States of America* 104.8, pp. 2579–84. ISSN: 0027-8424. DOI: 10.1073/pnas.0606604104. URL: http://www.pubmedcentral.nih.gov/articlerender.fcgi?artid=1815225\&tool=pmcentrez\&rendertype=abstract.

Tamayo, J. et al. (Nov. 2007). “Underlying mechanisms of the self-sustained oscillation of a nanomechanical stochastic resonator in a liquid”. In: *Physical Review B* 76.18,

p. 180201. ISSN: 1098-0121. DOI: 10.1103/PhysRevB.76.180201. URL: http://link.aps.org/doi/10.1103/PhysRevB.76.180201.